Interference-mediated synaptonemal complex formation with embedded crossover designation

Interference-Mediated Synaptonemal Complex Formation with Embedded Crossover-Designation

Liangran Zhang[1], Eric Espagne[2], Arnaud De Muyt[2, 3], Denise Zickler [2] and Nancy Kleckner*[1]

[1] Department of Molecular and Cellular Biology, Harvard University, Cambridge, MA 02138, USA

[2] Institut de Génétique et Microbiologie, UMR 8621, Université Paris-Sud, 91405 Orsay, France

[3] Institut Curie, 26 rue d'Ulm, 75248 Paris cedex 05, France

* Submitting Author

kleckner@fas.harvard.edu

phone: 1-617-495-4477

Short title: integrated spatial patterning of synapsis and crossover sites

Key words:

meiosis, recombination, synaptonemal complex, interference, spatial patterning

Abstract

Biological systems exhibit complex patterns, at length scales ranging from the molecular to the organismic. Along chromosomes, events often occur stochastically at different positions in different nuclei but nonetheless tend to be relatively evenly spaced. Examples include replication origin firings, formation of chromatin loops along chromosome axes and, during meiosis, designation of crossover recombination sites ("crossover interference"). We present evidence, in the fungus *Sordaria macrospora*, that crossover interference is part of a broader patterning program that includes synaptonemal complex (SC) nucleation. This program yields relatively evenly-spaced SC nucleation sites; among these, a subset is also crossover sites that show a classical interference distribution. This pattern ensures that SC forms regularly along the entire lengths of the chromosomes as required for homolog pairing maintenance and interlock sensing while concomitantly embedding crossover interactions within the SC structure as required for both DNA recombination and structural events of chiasma-formation. This pattern can be explained by a threshold-based interference process. This model can be generalized to give diverse types of related and/or partially overlapping patterns, in two or more dimensions, for any type of object.

Significance Statement.

Spatial patterns occur in biological and non-biological systems. A paradigmatic example occurs during meiosis. As shown a century ago, crossover recombination events occur at different positions in different meiotic nuclei; nonetheless, occurrence of a crossover at one position decreases the probability that another will occur nearby. As a result, crossovers tend to be evenly spaced. The current study suggests that this classical "crossover interference" is part of a broader program that concomitantly specifies even spacing of nucleation sites for formation of synaptonemal complex, a prominent meiotic chromosome structure. A model emerges for how the observed patterns could occur. This model provides a general explanation for the formation of complex, multi-layered patterns that is generally applicable to biological and non-biological systems.

\body

Introduction

Meiosis is the specialized cellular cycle that yields haploid gametes for sexual

reproduction. A central feature of the meiotic program is recombination (1, 2). DNA/DNA recombination interactions, initiated by programmed DSBs, mediate the recognition and juxtaposition ("pairing") of homologous chromosomes. A minority subset of these interactions mature into reciprocal crossover recombination products (COs) while the remaining majority mature primarily into inter-homolog noncrossover products (NCOs). COs promote genetic diversity but are also required for the segregation of homologous chromosomes (homologs) via their role in creating chiasmata (3).

A nearly-universal feature of meiosis is that COs occur along a particular chromosome at different positions in different meiotic nuclei but, nonetheless, along any given chromosome, tend to be evenly spaced. This pattern is a consequence of the fact that, if a crossover occurs at one position, there is a reduced probability that another crossover will occur nearby. Existence of such patterning was identified over a century ago as the genetic phenomenon of CO interference (4, 5).

A second central feature of the meiotic program is the synaptonemal complex (SC). This prominent structure links the axes of paired homologs along the lengths of the chromosome at the mid-prophase pachytene stage (3, 6, 7). In the canonical meiotic program, as shown in several organisms, CO patterning and SC formation occur concomitantly at zygotene (8; Discussion). Correspondingly, in budding yeast, the SC is not required for CO patterning (9, 10). Intriguingly, however, in two organisms, *S.pombe* and *A.nidulans*, SC and CO interference are concomitantly absent (3), pointing to some type of relationship between the two processes.

The present study began by investigating the possibility that the process of interference is not confined specifically to COs but instead acts more broadly to include SC nucleations. Such integration could concomitantly ensure regular SC formation along the chromosomes plus embedding of CO recombinational interactions in a specialized local relationship to the SC. To this end, we analyzed chromosomal events in the filamentous fungus *Sordaria macrospora*. Sordaria exhibits the canonical meiotic program and provides uniquely detailed readouts for recombination and SC formation including ultrastructural data from 3D serial section reconstructions and whole cell analysis of fluorescent signals for both recombination complexes and the SC as they evolve through prophase (8, 11-13). Our findings support the existence of a pattern in

which interference mediates regular spacing of SC nucleation sites, among which a subset comprises CO designation sites that exhibit classical interference.

We next investigated the possible mechanisms by which such a pattern might arise. The entire pattern, with all of its component features, appears to emerge during the same single stage, zygotene. Correspondingly, it is attractive to consider that the entire array arises in a single patterning process. Detailed analysis supports a mechanism in which SC nucleations, with embedded CO-designation, emerge via a single interference-mediated process. The basic principles that emerge are common to any interference-mediated patterning process and could, in principle, generate diverse complex interrelated patterns. The same principles apply equivalently to non-biological systems.

Results

Background. In *Sordaria macrospora*, cytological studies define a multi-step recombination process (8, 11; Fig. 1*A*). Throughout the process, recombination complexes are associated with chromosome structural axes and/or the SC, as in a variety of organisms (2, 14, 15).

Recombination is initiated by programmed double-strand breaks (DSBs). By late leptotene, the ~57 ± 6 Rad51-marked DSBs have evolved into a total of 75-80 inter-homolog recombinational interactions marked by meiotic helicase Mer3 and the MutS-homolog Msh4 foci (8, 11). These ensembles span closely-aligned late leptotene homolog axes, marked by opposing pairs of foci of Mer3 (11) and a linking DNA segment. While turnover of Rad51 foci cannot be assessed, this numerology suggests that, while some DSBs likely yield inter-sister interactions as in other organisms, this outcome is relatively infrequent.

During zygotene, when SC is forming along the homologs, all recombinational interactions lose their Mer3 foci and develop foci of Msh4. Concomitantly, these total interactions are undergoing differentiation into three types, as revealed by integration of these patterns with findings from ultrastructural studies (8, 13).

(a) ~22 interactions are designated for eventual maturation into COs. These interactions are marked by the presence of large SC-associated nodules (so-called "late nodules" or "LNs"), which emerge at zygotene. By early-pachytene, when SC is formed all along the chromosomes, LNs occur in the same number and distribution

as mid-late pachytene Hei10 (T3) foci, diplotene chiasmata and COs assayed genetically (discussion in ref. 8). Thus, CO-designation and interference have arisen no later than zygotene. [We note that the above correspondences suggest that, in Sordaria, the vast majority of all COs arise via programmed CO-designation/interference, with relatively few arising in other ways, e.g. as so-called "non-interfering COs" (16).]

(b) A similar number of interactions are marked by a second, smaller type of SC-associated nodule, so-called "early nodules" ("ENs"). ENs also emerge at zygotene, concomitant with LNs (13). LNs and ENs are referred to together as "recombination nodules" or "RNs".

(c) The remaining ~30 interactions are not marked by any nodule. Their existence is inferred from the fact that the total number of LNs and ENs is less than the number of Mer3/Msh4 foci at leptotene/zygotene and because an appropriate corresponding subset of Msh4 foci exhibits a unique temporal pattern, unique absence of colocalization with Hei10 T2 foci, and unique functional dependence on Hei10 (8).

These three types of interactions then further evolve. At early pachytene, the subset of RN-marked interactions (ENs plus LNs) are also marked by ~40 medium-sized foci of the structure-based signal transduction protein Hei10 (so-called Hei10-T2 foci). The number of T2 foci and the sum of ENs plus LNs are identical, indicating that interactions not marked by a nodule do not develop such foci. At mid-pachytene, the two types of RN-marked interactions exhibit different maturation fates. ENs and their corresponding Hei10-T2 foci disappear. LNs, in contrast, persist to later stages (diplotene) and their Hei10-T2 foci evolve into (even larger) Hei10-T3 foci. Interactions not marked with a nodule or a Hei10 focus also progress, more rapidly than the nodule/Hei10-marked interactions, as shown by earlier loss of Msh4 foci (8).

Ultimately, EN-marked and non-nodule-marked interactions both progress, likely primarily to non-crossover (NCO) products, as implied by genetic analysis (13; discussion in ref. 8) (probably not to inter-sister or "non-interfering COs"; above). Thus, according to these patterns: (i) ENs and LNs develop T2 foci but have different DNA fates; in contrast, (ii) ENs and non-nodule-marked interactions are, by definition, morphologically non-congruent; nonetheless both give NCO products (Fig. 1*A*).

Hypothesis. Sordaria CO recombination sites exhibit classic CO interference (8, 13). Interference can be accurately defined by Coefficient of Coincidence (CoC) analysis

(17). In brief, chromosomes are divided into intervals; for each pair of intervals, the frequency of chromosomes exhibiting a CO in each interval ("double CO") is determined and compared with the frequency predicted for independent occurrence of COs in the two intervals. The ratio of these values (observed/expected) is the CoC. For intervals that are close together, the observed frequency is less than that predicted, to increasing extent with decreasing inter-interval distance, reflecting interference. At closely-spaced intervals, double COs are essentially absent. In Sordaria, CO interference is exhibited by the distributions of both LNs and Hei10-T3 foci (Fig.1*B*). A convenient metric for the apparent strength of interference is the inter-interval distance at which CoC = 0.5 (L_{COC}). For both LNs and Hei10-T3 foci, L_{COC} = ~1.3μm as judged by CoC curves that include all regions of the genome. LNs appear during zygotene and exhibit their final interference distribution by early pachytene, implying that CO patterning in Sordaria must occur no later than zygotene (8; above). Since a full array of total Mer3-marked recombinational interactions is observed at late leptotene (8, 11), CO site designation and interference likely arise during zygotene and thus concomitant with SC formation.

In Sordaria, as in other organisms, SC formation is specifically nucleated at sites of recombinational interactions (10). Functional studies further show that nucleations occur at only a subset of total interactions (19). Moreover, ultrastructural studies show that short segments of SCs often have an associated LN and/or EN (13). This feature raised the general prospect that SC formation might nucleate specifically at sites of interactions that are being designated to develop LNs and ENs, concomitant with LN/CO patterning. Recent analysis has further revealed that the array of total RNs, and of their fluorescence correlate Hei10-T2 foci, also exhibit interference, with L_{COC} = ~0.6μm (8; Fig. 1*C*). Thus: if total RNs indeed mark the sites of SC nucleations, then SC nucleations would also exhibit interference, and a tendency for even spacing (Introduction). Moreover, the sites of CO-fated recombinational interactions would be embedded within this array, at a subset of nucleation sites, with a classical CO interference distribution (Fig. 1*D*).

A 1:1 Relationship Between SC Nucleations and RNs (ENs+LNs)/T2 Foci. To test the above hypothesis, we analyzed in detail the relationship between SC segments and RNs (LNs and ENs) using data from 3D EM reconstructions (13; Fig. 2*AB*). Analysis was performed on all bivalents 1 and 2 from 60 serially sectioned zygotene nuclei. Among Sordaria's seven bivalents, these two are the longest and most easily identified;

moreover, bivalent 2 is distinguished by the fact that one end is embedded within the nucleolus.

Traced chromosomes were divided into categories on the basis of SC and RN patterns (Fig. 2*C*). (I) Early zygotene bivalents exhibit short SC segments. Most segments exhibit a single associated LN or EN, which, in many cases, is located at the end of the associated SC segment. Some SC segments have no associated RNs ("solo SCs"). (II) As zygotene progresses, short segments tend to exhibit a single RN located internally, rather than at one end; some segments exhibit more than one nodule; and solo SCs also occur but are more rare than at early zygotene. (III) Early pachytene nuclei exhibit a full complement of LNs and ENs (8, 13; below). (IV) Mid/late pachytene nuclei exhibit only LNs, present in full complement, reflecting precipitous loss of ENs at the early/mid-pachytene transition (8, 13).

For the present analysis, we concentrated on the relationship between SC segments and RNs as they emerge coordinately during zygotene. To characterize potential nucleation segments, we analyzed short SC segments containing zero, one or two RNs. A clear progression emerges (Fig. 2*D*). Solo SCs (lacking any RN) are uniform in length and are very short, 0.2-0.3μm. Segments with a terminal nodule are longer than solo segments and segments with internal nodules are longer than segments with terminal nodules. Moreover, LN-associated SC segments are significantly longer than EN-associated segments in both categories. These patterns suggest a specific sequence of events (Fig. 2*E*): (i) an "event designation" occurs at the site of a recombinational interaction, triggering emergence of a short SC segment which extends in one direction from the designation position; (ii) a nodule soon emergences at the designation site, preceded/accompanied by continued SC elongation; finally, (iii) SC elongates symmetrically in both directions.

The regularity of this pattern is confirmed by consideration of SC segments that exhibit two associated nodules, which occur in several configurations according to the types and positions of their nodules (Fig. 2*F*). The lengths of these different configurations are proportional to the lengths predicted from the sums of their two component nodule/SC segments, with the addition of a modest increase in SC length relative to the reference values (Fig. 2*G*).

These results provide strong support for a 1:1 relationship between SC nucleations and RN [EN+LN] formation and thus, by extension, for the patterning hypothesis proposed above. These results also provide two additional pieces of

information.

(i) SC initially forms asymmetrically, in one direction away from its designation/nucleation site, as previously suggested (13). One possibility is that asymmetry is dictated by the recombination complex at the initiation site, where one DSB end has invaded a D-loop to give an asymmetric disposition of component features (1). SC formation is concomitant with D-loop extension (1). Perhaps the SC initially spreads in the same direction as the growing D-loop in order to ensure that the developing recombination complex is well-associated with the forming SC. Or, oppositely, the SC might spread specifically in the opposite direction so that the structure can maintain a robust inter-homolog axis connection at developing CO sites despite the presence of an active recombination complex.

(ii) LN-associated SC stretches are longer than EN-associated SC stretches. This distinction confirms that both of the corresponding types of interactions play nucleating roles and further demonstrates that the two types of nucleations are qualitatively distinct. It remains to be determined whether longer LN-associated SC stretches reflects earlier SC nucleation at those positions or an intrinsic difference in underlying molecular events. Such a difference could relate to the fact that CO sites (and thus LNs) must be integrally embedded within the SC whereas ENs are less robustly associated and are lost from the SC at early pachytene, e.g. as part of a program to dissociate nucleation-associated recombinational interactions from the structure (Discussion).

A Threshold Designation Model for Complex Interference-Mediated Patterning. Since the array of SC nucleations and the embedded array of CO-designated sites arise contemporaneously, it is simplest to suppose that both features arise as part of a single patterning process. How could such a process occur?

A general outline of a possible scenario is as follows (Fig. 3*A*). Event-designation occurs progressively, operating on an array of undifferentiated precursor interactions, and driven by some particular molecular change. Regardless of the underlying basis for this change, a critical feature will pertain: each designation is accompanied by spreading interference which, by its intrinsic nature, will tend to reduce the "reactivity" of affected remaining precursors. Consequently, as the process progresses, the local reactivity of the particular precursor that happens to undergo designation at a given moment will be highest for the first designations and will tend to

become lower and lower as the process progresses. Finally, the reactivity is sufficiently low that no more designation events occur (Fig. 3*A top*). This scenario opens up the possibility that, as the designation process progresses, the molecular outcome of an event might change, in relation to the decreasing local reactivity of the available precursors (Fig. 3*A top*). Initially, when local reactivities are higher, designation would give one type of outcome. When reactivity falls below a certain threshold, another type of outcome might occur. In principle, any number of such thresholds could come into play sequentially during the designation process. Given multiple thresholds, diverse combinatorial patterns could be generated (Discussion).

Given only two thresholds, three types of patterns will be produced: the two types arising in the two phases and the total of all designation events (Fig. 3*A bottom*, pink, brown and black, respectively). Event patterns in Sordaria could be described in this way: both types of designation would yield SC nucleations; however, only the first type would concomitantly yield CO-designation (and an LN) while the second type would not be CO-designated and would yield an EN (below).

The above idea emerged from, and can be further described and evaluated in the context of, the beam-film (BF) model for interference (9, 17, 20, 21). By this model, patterning begins with an array of precursors (e.g. late leptotene total DSB-mediated inter-homolog interactions, as seen for Mer3 foci in Sordaria (11). This array of precursors undergoes a sequential designation process. All interactions come under mechanical stress until a first (more stress-sensitive) interaction goes critical, undergoing a stress-promoted change in state that commits it to the CO fate ("CO-designation"). That event, by its nature, alleviates stress locally at the site of the change. Because of the mechanical nature of the system, this local change (reduction) in stress then redistributes outward in both directions, dissipating with distance. The resultant reduction in stress automatically reduces the probability of subsequent stress-promoted events in the affected region, most strongly near the nucleation site and to a lesser extent with increasing distance away from that site. A next designation event may then occur. If so, it will occur preferentially in unaffected regions. If events then occur, each of these will tend to occur away from the positions of prior events, thus generating even spacing and interference. Designation events continue to occur until none of the remaining precursors is any longer sensitive to the level of global stress.

The outcome of such a process can be simulated mathematically as a function of key parameters relating to the nature of the precursor array, the patterning process *per*

se and the efficiency with which a designated event actually matures into a detectable signal. Simulations of experimental data by this model can very accurately describe CO patterns in wild-type and mutant budding yeast, Drosophila, tomato and grasshopper (9, 17; e.g. for budding yeast, Fig. 3*BCD*) and Sordaria (below).

In such simulations, progressive event designation is achieved by a particular computational device: all parameter values are held constant and the level of global stress is increased, step by step, after each designation event, with the final number of events specified by the maximum global stress level (Smax). In reality, the same effect could be achieved in other ways. In the context of the stress model, the same outcome would be achieved equivalently by a progressive globally increase in the sensitivity of precursors to a fixed level of stress. Alternatively, the global stress level could be constant, with designation events occurring sequentially in time as a function of their local stress level at that moment.

Importantly, the predictions of the BF model will apply equivalently to any patterning process that exhibits the same basic logic: sequential event designation with each designation event triggering an inhibitory effect that dissipates exponentially in both directions away from its nucleation site.

The effects of progressive event-designation are illustrated by BF simulations using basic parameter values derived from budding yeast (Fig. 3*BC*) and convenient increasing values of Smax. As the process progresses, more and more designation events are forced into a given length of chromosome, resulting in more and more closely spaced events. Correspondingly, the CoC curve shifts to the left (Fig. 3*E*) while the number of designated sites concomitantly increases (Fig. 3*F*). Notably, this progression gives the same qualitative effects as progressive reduction in the strength of interference whereas, in fact, there is no such change: the interference signal exerts its effect over the same distance throughout the progression (L_{BF} = 0.3; Fig. 3*B*). The only change is a progressive increase in the fraction of precursor sites that have undergone event-designation (discussion in ref. 17). We further note that, as more and more designation events occur, the distribution of distances between adjacent events also changes. In general the value of the gamma shape parameter ν, sometimes used as a metric of the tendency for even spacing (and thus interference), decreases (17).

This progression can also illustrate the consequences of a thresholded designation process. We consider two particular threshold values of Smax (Fig. 3*G*). Up to a first threshold, one type of designation outcome occurs (Type 1; pink) and a further

increase to a second threshold gives a second type of outcome (Type 2; brown), giving a final array of events comprising the sum of the two (Total; black). The three sets of events are characterized by different average numbers and distributions of events (Fig 3*H*); different CoC relationships (Fig. 3*I*); and different distributions of distances between adjacent events with correspondingly different values of the gamma distribution evenness parameter ν (Fig. 3*J*).

The overall result of these events is a partially overlapping pattern of event-designations in which a total array of relatively evenly-spaced events (black) contains two embedded individual arrays (pink and brown), each of which also exhibits an interference distribution (Fig. 3*K*). This theoretical example illustrates the fact that, qualitatively, such a two-threshold scenario could explain the pattern of events seen along Sordaria chromosomes. A first set of event-designations would concomitantly give both SC nucleation and CO-designation (pink/black). Then, beyond a particular threshold of reactivity, further designations would still give SC nucleation but would no longer concomitantly give CO-designation (brown/black). The result would be a larger array of relatively evenly-spaced SC nucleations, within which is embedded a smaller array of CO-designation events that exhibit a classical interference distribution.

Experimental Event Patterns Match those Predicted for a Single Interference-Mediated Patterning Process. In the above model, the pattern of events observed along Sordaria chromosomes would arise in a single interference-mediated process that operates on an original starting array of precursor events, with a single set of basic patterning "parameters" operating throughout. In an obvious alternative model, the observed pattern of events would arise in two independent sequential processes: a first round of interference would operate on the original starting precursor array, with one set of patterning parameters; then a second round of interference would operate on the array of events produced by the first round, characterized by a second set of patterning parameters. This scenario is not attractive *a priori*, given that LNs, ENs and SC nucleations all arise concomitantly during zygotene. However, a unique feature of Sordaria recombination patterns makes it possible to distinguish between these two scenarios.

In Sordaria, the pattern of total recombinational interactions present at late leptotene is very well defined by the patterns of Mer3 and Msh4 foci (8, 11). These total interactions are quite regularly spaced, at an average distance of 0.6μm, with a value of

the gamma evenness parameter of >200 (11; Fig. 4*i top*). During any interference process that operates on this total array of interactions, as more and more designation events occur, those events will tend to be closer and closer together and thus, ultimately, will tend to occur at adjacent precursor sites. Since these precursor sites are very evenly spaced (above), the array of distances between adjacent events should tend to exhibit a peak specifically at the inter-precursor distance (0.6μm). Moreover, that peak should be more prominent for bivalents that have acquired more events relative to total bivalents. Exactly such a peak, which is more prominent in bivalents with more events, is observed in the experimental data sets for T2 foci, which represent total event-designations/SC nucleations (Fig. 4*i, middle*). This is expected for both the one- and two-round(s) of interference scenarios, which give the same final total array of events that all arise from the original total array of precursor sites. Remarkably, however, exactly the same peak is also seen for T3 foci, which represent only the sites that have undergone both CO-designation and SC nucleation (Fig. 4*iii, middle*). This result provides a strong indication that T3 foci arise from the array of total precursor interactions, as predicted by the one-round scenario. If T3 foci had arisen instead from the array of T2 foci, there would have been a tendency, instead, for closely-spaced double T3 foci to be separated by the distance between adjacent T2 foci (further discussion below).

The effects of these tendencies are also apparent in CoC curves. Double event bivalents, in which two events have occurred in different intervals along the same chromosome, are very rare at small inter-interval distances. Correspondingly, for events that arise directly from the original precursor array of total interactions, closely-spaced double events will tend to occur specifically at the inter-interval distance corresponding to the distance between adjacent interactions (~0.6μm). This tendency is predicted to appear as a "hump" in the CoC curve at the appropriate position. Such a hump is discernible as a shoulder in the CoC curve for T2 foci; more tellingly, it is also a prominent discrete feature of the CoC curve for T3 foci (Fig. 4*i, iii, bottom*).

BF best-fit simulation analysis confirms and extends these conclusions.

- We first defined the best-fit simulation match for the T2 focus pattern (total events) as they arise from the initial precursor array of total recombinational interactions. As described in the example above (Fig.3*G*, "Total"), this match defines all BF parameter values, most notably the interference distance (L_{BF} = 1μm) and the value of Smax for total events ($Smax_{total}$=4.5). The best-fit simulation for T2 foci accurately

describes both CoC relationships and the average number and distribution of events (Fig. 4*ii, bottom*). It also recapitulates the tendency for adjacent T2 events to occur preferentially at the average inter-precursor distance by all of the criteria above, with a peak at the appropriate position in the distribution of inter-event distances, and a corresponding shoulder in the CoC curve (Fig. 4*ii, middle and bottom*). Additionally, recapitulation of this tendency requires that precursors tend to be evenly spaced; no such tendency is observed if precursors are assumed to occur randomly along the chromosomes (Fig. S1).

- If the one-round threshold mechanism pertains, it should now be possible to identify, without changing the values of any other parameters including L_{BF}, a value of Smax that is lower than $Smax_{total}$ at which the number and distribution of designation events matches those of T3 foci (as illustrated by Fig. 3*G*, "Type 1"). In fact, such a value can be obtained at $Smax_{T3}$=1.8 (Fig. 4*iv, bottom*). Importantly, this simulation also recapitulates the tendency for adjacent T3 events to occur preferentially at the average inter-precursor distance by all of the criteria above as seen in both the distribution of inter-event distances and the CoC curve (Fig. 4*iv, middle and bottom*). And, as for T2 foci, recapitulation of this tendency requires that precursors tend to be evenly spaced (Fig. S1).

- In contrast, if the two-round mechanism pertains, it should be possible to use the array of T2 foci as the precursors for a second, independent round of interference, which yields appropriate T3 focus patterns. The best-fit simulation of this scenario does, in fact, provide reasonable matches between experimental and predicted data with respect to CoC curves and the number and distribution of designated events (Fig.4*v, bottom*). However, there is no tendency for adjacent events to be separated by the distance corresponding to the distance between total starting recombinational interactions, nor is there any indication of a "hump" at the corresponding position (Fig. 4*iv, middle and bottom*). This simulation confirms that the two rounds do not adequately explain the experimental data, in the particular way that specifically distinguishes between the one- and two-round cases.

To further understand the nature of the closely-spaced double events seen for T2 and T3 foci, we further inspected the patterns along each analyzed chromosome in the experimental data sets. Interestingly, for both T2 foci and T3 foci, the majority of closely-spaced double events tend to occur near the chromosome ends (70 pairs among 117 pairs of T2 foci; 18 pairs among 28 pairs of T3 foci). This tendency is likely related to the

fact that SC initiations, ENs and LNs all tend to occur first near chromosome ends (13; Fig. S2). BF best-fit simulation of the one-round scenario also captures this feature of the data. In the stress hypothesis, the status assigned to the chromosome ends will influence the probability of event-designations in nearby ("sub-telomeric") regions. If a chromosome end is free ("unclamped"), it will not support stress and thus will behave as a pre-existing designation event, thus disfavoring near-end events. Oppositely, a "clamped end" will support stress and favor near-end events because interference will emanate across sub-terminal positions only from internal regions and not from beyond the end of the chromosome (17, 20). [*In vivo*, clamping could correspond to association of a chromosome end with the nuclear envelope; however, outside of the stress hypothesis, the clamping parameter simply provides a convenient way to modulate the probability of events near ends.] In best-fit BF simulations of T2 and T3 foci by the one-round scenario, occurrence of closely-spaced double events near chromosome ends requires that both ends be clamped (in accord with nuclear envelope association of ends at this stage as defined by EM (Fig. S2; 13)). We also find that longer bivalents exhibit very few double events, at any position, for reasons that are presently unclear. Correspondingly, the above analysis considers only the shorter bivalents, 3-7, which are evaluated as a single group.

In summary: above considerations suggest that the observed pattern of SC nucleations with embedded CO interference are well explained by a single round of interference with thresholded designation, first of SC nucleations and accompanying CO-designations (and LNs) and then of more SC nucleations without accompanying CO designations (and ENs). Of course, in real chromosomes, these are probabilistic tendencies that need not comprise an absolute temporal sequence. However, we find experimentally that SC segments with an associated LN tend to be longer than SC segments with an associated EN. While other explanations are not excluded, this is the pattern expected if the LN-associated segments tend to be nucleated earlier in zygotene than the EN-associated segments, i.e. if SC nucleations with associated CO-designation tend to precede SC nucleations without CO-designation. It is also true that LNs and ENs themselves appear concomitantly during zygotene, rather than sequentially. However, this timing reflects not only the time of designation of the corresponding sites but also the time required for appearance of a visible nodule. Thus LN site-designation could occur earlier, as suggested by SC length comparisons, but with a longer time required for development of a visible LN versus a visible EN.

Alternative Models. We have attempted to identify other models that could explain the observed event patterns. Experimental data do not appear compatible with a two-round scenario in which all SC nucleation sites are designated in one round of interference-mediated patterning, with CO/LN/T3 sites then designated from among those interactions in a second round of interference (above). A related two-round model would suggest that total SC nucleations (T2 foci) would first occur at a random subset of total recombination sites, with CO-designation then occurring at a subset of those sites by an interference-mediated process. This model is also not possible: by this scenario, the distribution of T2 foci would match the distribution of total recombination sites, which is not the case (Fig. S3).

Other types of two-round models could be envisioned in which LN- and EN-correlated designations occur sequentially, by two independent interference processes, but with both types arising from the set of total recombinational interactions. SC nucleations with CO-designation might occur first, by one interference process, followed by SC nucleation without CO-designation acting on remaining "unreacted" precursors by another process. Oppositely, SC nucleation without CO-designation might occur first, followed by SC nucleation with CO-designation acting on remaining precursors.

Another type of scenario would suppose that SC nucleations accompanied by CO-designation and SC nucleations that are not accompanied by CO-designation occur simultaneously by two independent interference processes. Such a mechanism would require rules for what happens if both processes encounter the same precursor site.

None of these three models has the same economy and simplicity as the threshold mode. However, they cannot presently be excluded.

Discussion

Interference-Mediated SC Nucleation with Embedded CO-Designation. The presented analysis of RN and SC patterns in 3D reconstructed nuclei point strongly to a 1:1 relationship between total RNs (ENs+LNs) and SC nucleation sites. We previously showed that total RNs (and corresponding Hei10-T2 foci) are relatively evenly spaced in an interference pattern while LNs (and corresponding Hei10-T3 foci) mark the sites of CO-fated recombinational interactions (8). Taken together these findings imply that zygotene chromosomes exhibit a relatively evenly-spaced array of SC nucleations with

embedded CO sites that exhibit classical CO interference. Consideration of events in other organisms suggests that this pattern is likely to be quite general, as discussed in detail below.

This observed pattern is biologically quite attractive because it concomitantly satisfies the distinct requirements of the SC for its global roles along the chromosomes and for its local roles at the sites of CO recombination.

- Continuous SC along the lengths of the chromosomes is a nearly ubiquitous feature of the meiotic program. Total recombinational interactions link homologs along their lengths through late leptotene, via their associations with axial structure (11). However, by early/mid-pachytene, only CO-fated interactions remain axis/SC associated (8, 13; discussion in ref. 22; below). Thus, full length SC is required to keep homologs together at/after this point. This requirement is particularly stringent in organisms with very few COs. This is especially true when those few COs are always near the ends of the chromosomes and, most dramatically, in some higher plants where, in addition, the chromosomes are extremely long (e.g. 23, 24). The tendency for evenly-spaced SC nucleations ensures that SC forms efficiently and regularly along the chromosome lengths as required for this role. Additionally, SC formation *per se* appears to mediate the sensing of chromosome interlocks (11), a role that also requires multiple well-spaced initiations along the chromosomes.

- CO recombination and the SC undergo local functional interplay in both directions. The structural constraints of the SC may stabilize the recombination ensemble against biochemical turbulence. Recombinosome/SC relationships could also provide the geometric constraint required to direct the resolution of double Holliday junctions specifically to CO products, rather than to NCO products or to a mixture of the two (1, 25). Additionally, CO sites ultimately mature into chiasmata, which involves local structural changes (e.g. "crossing-over" at the level of chromosome axes). Cytological studies implicate local SC and associated recombination complexes in these processes as well (26, 27).

The current findings are also of interest because they bring the meiotic crossover interference process, previously considered to apply only to patterning of recombination sites, into a general chromosomal context. Crossover interference is thereby linked to basic chromosomal phenomena in which a tendency for even spacing is known or suspected, e.g. DNA replication initiation, chromatin loop formation or formation of inter-sister linkages (20, 28). This, in turn, further encourages interference mechanisms in

which transmission of information occurs via chromosome structural features, as suggested by recent studies in budding yeast (9), rather than solely involving effects targeted to recombination complexes alone.

Sordaria Zygotene Chromosomal Patterns Appear to Arise Via a Single Interference-Mediated Process. Available evidence suggests that SC nucleation and CO-designation occur contemporaneously during zygotene (above). Detailed analysis of these events, as reflected in the patterns of Hei10 T2- and T3-foci, provide evidence that both features arise via a single interference-mediated process. (i) SC nucleations (T2 foci) and CO-designations (T3 foci) both arise from the array of total recombinational interactions defined for late-leptotene chromosomes. (ii) BF best-fit simulations of a single interference process can very accurately describe the observed experimental outcome. (iii) BF best-fit simulations argue strongly against emergence of the observed patterns via two sequential rounds of interference, both occurring during zygotene, with one process acting on total interactions to yield SC nucleations and a second process acting on the array of SC nucleations to give a final pattern of CO-designated sites. (iv) Other models that we have been able to envision are either incompatible with the data in principle, cannot give an appropriate outcome in BF simulations, and/or involve multiple *ad hoc* assumptions.

Complex Spatial Patterns can Arise in a Single Interference-Mediated Process Via Event-Designation Thresholding. The basic logic of CO interference is very well-described by the logic of the BF model, irrespective of whether a mechanical mechanism is involved or not (9, 17). By this logic, interference is intrinsically characterized by a basic progression. Every designation event triggers spreading interference, which reduces the reactivity of all affected precursor interactions. As a result, as more and more precursor events undergo event-designation, the less and less reactive the remaining precursors become to the designation process. The current study has elicited the possibility that this feature has previously unappreciated potential implications: if the molecular outcome of designation is sensitive to the reactivity of the precursor involved, then that outcome can change progressively as the process proceeds.

Many types of patterns can be envisioned *a priori.* In the case at hand, the process is defined by only two "thresholds" for event-designation, with an overlapping effect. Zygotene chromosome patterns are explained if early designations give SC

nucleation plus CO-designation, with attendant intimate linkage of recombination and structure, whereas later designations give only SC nucleation. Morphologically, as seen at early pachytene, the first set of events also give LNs; the second set of events also give ENs; and all events give T2 foci. In principle, a patterning process could involve any number of different thresholds with diverse, combinatorial overlappings. Thus, this simple basic premise could potentially underlie and explain very complex patterns.

We note that the predictions of the thresholding scenario for SC nucleation and CO-designation can be very smoothly integrated with our previous proposal for how CO interference might occur (9, 20, 21). In fact, we can now appreciate that our model directly predicts the observed graded effect.

- We have proposed that global chromatin expansion places the structural axis meshwork of late leptotene chromosomes under mechanical stress. As a result, all local inter-axis recombination complexes are under stress. That stress provokes changes that cause certain complexes to change into a CO-designated form. That change, in turn, alleviates local stress, implying local chromatin compaction. And that local compaction, in turn, licenses local SC installation, giving nucleation at CO sites. Global compaction at the end of zygotene then permits filling-in of SC between nucleation sites. The need for such an effect is shown directly in Sordaria where each SC nucleation only spreads for a limited distance along the chromosomes (19). This overall pattern also fits with the fact that leptotene is specifically characterized by chromatin expansion whereas zygotene is specifically characterized by chromosome compaction (20). Indeed, even in *C. elegans*, where CO interference occurs after SC formation, recent findings imply that the chromosomes are under chromatin expansion stress due to constraints of the SC, in accord with a role for expansion stress in CO-designation (29).

- In the context of this proposed model, it is easy to envision that, as the designation/interference process progresses, local precursor reactivity will be insufficient to give CO-designation; however, if interference implies decreased chromatin expansion, SC nucleation will be progressively favored as the process progresses, thus permitting/promoting a continued designation process that gives SC nucleations without accompanying CO-designation, exactly as implied by the current analysis.

Interference-Mediated SC Formation, with Embedded CO-Designation: Generality. The pattern described here for Sordaria may well be very general among

organisms that exhibit the "canonical" meiotic program.

Plants and mammals. In tomato, a large population of ENs emerges during zygotene, specifically at sites of SC nucleation (30): they are seen specifically at convergences (which are known to be sites of SC nucleation in this and other plants; e.g. 3; 31) as well as synaptic forks. Moreover, they do not emerge on already-formed SC (30). These ENs tend to be evenly spaced as shown by gamma distribution analysis of inter-EN distances (31), implying that SC nucleation sites also exhibit such a distribution and thus are subject to an interference process. Importantly, this tendency for even spacing is true not only in tomato (31) but analogously in many higher plants, implying broad generality. It has been suggested for tomato that these ENs are precursors to LNs (32), with the further implication that one round of interference occurs to give the EN distribution and that CO-designation then occurs during pachytene, in a "second round" of interference that operates on the EN-marked complexes (e.g. 31). This suggestion emerges from the fact that ENs are seen at zygotene and early pachytene; then, at early/mid-pachytene most of these nodules precipitously disappear and a few CO-correlated larger nodules (LNs) emerge (e.g. 32). However, Mlh1 foci, which are specifically diagnostic of "interfering COs" are seen already at zygotene in tomato (31). Moreover, biochemical studies of ENs in tomato show that a subset of the many early pachytene nodules are physically more strongly associated with the SC than others (33), with the number and distribution of that subset of stably-associated nodules matching the number and distribution of later large CO-correlated LNs. Both of these findings suggest that, in fact, CO-designation occurs at zygotene, as in Sordaria. Moreover, precipitous loss of ENs at early pachytene is not diagnostic of a second round of interference: it is seen also in Sordaria and thus well after CO-designation has occurred (above).

It has also been proposed for mouse that interference arises in "two rounds" (34). Again, one round of interference would operate during leptotene/zygotene on total recombinational interactions to yield a number of recombination complexes intermediate between the number of DSBs and the number of COs. A second round of interference would then operate during early/mid-pachytene, on the events generated in the first round, to give the final array of COs. For this organism, the two-round proposition emerges from the finding that an "intermediate number" of Msh4 foci occur on early/mid-pachytene chromosomes and that Mlh1 foci, which specifically mark the sites of interfering COs, emerge at mid/late pachytene. However, exactly these same patterns

are seen for Msh4/Hei10-T2 foci and Mlh1/Hei10-T3 foci in Sordaria, where CO-designation is completed before early pachytene (8; above). Specifically: (a) In Sordaria, an intermediate number of recombinational interactions are marked at early/mid-pachytene by Hei10-T2 foci, and these interactions already include CO-designated sites that show interference as a result of the events of zygotene. (b) These early/mid-pachytene T2 foci are also marked by a corresponding specific intermediate number of Msh4 foci, thus exactly corresponding to the intermediate number of Msh4 foci seen in other organisms. (c) Hei10-T3 foci emerge at mid/late pachytene where, by all available criteria, they correspond to the Mlh1 foci that emerge at this stage in all organisms tested so far. Thus, the basic findings upon which the "two-round" scenario is based can be explained just as easily by the one-round zygotene scenario seen in Sordaria. Notably, also, in mouse, Msh4 foci and SC nucleations strongly colocalize at zygotene, consistent with earlier specification of Msh4 focus patterns in local coordination with SC nucleation (35,36).

Analogously, in human, inter-homolog bridges of recombination protein RPA occur in a number intermediate between total DSBs and COs (37) and, in this organism, CO-correlated LNs are morphologically visible at zygotene (38), just as in Sordaria.

It can be further noted that an "intermediate number" of Msh4 foci is seen also in Arabidopsis, with the same potential Sordaria-analogous interpretation as in mouse.

In summary: all available evidence is consistent with the existence of a single round of interference that gives rise to evenly-spaced SC nucleations with concomitant embedded CO-designation, not only in Sordaria but also in plants and mammals. By this view, different organisms differ only with respect to: (i) the extent to which and/or timing with which CO-fated interactions develop morphologically distinct features at zygotene (rather than later) and (ii) the proportion of SC nucleations that are CO-fated, which is higher in Sordaria, intermediate in mammals and lowest in plants.

Budding yeast. Budding yeast provides an interesting "exception that proves the rule". In this organism, CO-designation and interference are known to occur prior to and independent of SC formation, which is then nucleated as a downstream consequence at CO-designated sites. These conclusions emerge from the following findings. (a) CO-correlated Zip2/3 foci exhibit an interference pattern that arises independent of the SC central region component Zip1 (9, 10). (b) CO-specific DNA intermediates arise at leptotene/zygotene, dependent on Zip1, implying that CO-designation precedes or is concomitant with SC nucleation (21). (c) Zip2/3 sites mark not only sites of COs but

also sites of SC nucleation (10). This relationship has two important implications. First, CO-designation and SC nucleation are directly linked. Second, there is a 1:1 relationship between the two events: every SC nucleation is a CO-designation and every CO-designation is an SC nucleation. Thus, in this case, the more general pattern pertains, but in an extreme form where there are no "extra" SC nucleations beyond those corresponding to CO-designation sites. Correspondingly, ENs (which mark the positions of extra SC nucleations in Sordaria) have not been observed in budding yeast. Moreover, in Sordaria and other organisms, Msh4 foci occur at mid-pachytene in an "intermediate" number corresponding to total SC nucleations (above); in contrast, in budding yeast at this stage, the number of Msh4 foci corresponds to the number of specifically-designated COs (~90; ref. 9; Figure 6 of ref. 39). This situation makes perfect sense in light of the fact that yeast chromosomes are not only very short but also exhibit a much higher density of COs per SC length than other organism. Thus, there is no need for extra nucleations to ensure full SC formation.

Non-canonical programs. In *S. pombe* and *A. nidulans*, CO interference and SC are both absent. This was long cited as evidence that the SC participates in interference, which is not true in yeast, mouse or Drosophila or, on the basis of timing, in Sordaria or human (above). The present observations provide a sensible possible rationale: if CO interference arises primarily to promote regular SC formation, then in the absence of SC, there will be no need for interference.

Different considerations pertain in the "non-canonical" meiotic programs of *C. elegans* and Drosophila. In these organisms, SC formation is independent of recombination and CO designation; moreover, recombination initiation and interference is/can both be implemented after SC formation (40-43). In these cases, the interference process seems limited to patterning of COs and not SC nucleation, suggesting a rationale for interference that relates to CO/chiasma formation (27). Notably, however, in *C. elegans*, recombination-dependent SC formation can be observed in certain circumstances (44).

Why ENs? The patterns of SC nucleations, ENs and LNs in Sordaria and other organisms (above) raise an interesting conundrum. LNs are robust, ultrastructurally-visible features and their prominence can be attributed to the need for robust association of CO-fated recombination complexes with the SC. But why do ENs exist? They are not involved in CO-specific events. Moreover, genetic evidence in Sordaria suggests that all non-CO-designation interactions are matured to non-crossover (NCO) products,

including both EN-marked and non-nodule-marked interactions. Thus, ENs are apparently not required to give an NCO outcome. The same could well be true in many organisms, since ENs always occur in an "intermediate number", greater than the number of COs but fewer than the number of DSBs. The sole distinguishing feature of ENs appears to be that they mark the sites of SC nucleations that will not progress to a CO outcome. SC nucleation involves an intimate association of the recombination complex with SC components. For example, in Sordaria, Mer3 and Msh4 foci go from on-axis to in-between axis positions exactly concomitantly with SC nucleation (11, 12). However, once nucleation is achieved, at nucleation sites that are not fated to become COs, persistence of this association is unnecessary and/or deleterious. We propose that ENs (and T2 foci) are required to mediate the surgical dissociation of the corresponding (NCO-fated) recombination complex from the SC. Further, we suggest that this dissociation is triggered by Msh4-mediated progression of the associated recombination complexes. This possibility is suggested by the fact that in Sordaria (8), ENs and the corresponding subsets of Hei10-T2 and Msh4 foci, disappear from the chromosomes concomitantly and abruptly at the early/mid-pachytene transition. This role would similarly rationalize the precipitous loss of ENs and/or Msh4 foci at early/mid-pachytene in plants, human, mouse and Sordaria; the existence of intermediate numbers of Msh4-containing recombination complexes in Sordaria, mouse and Arabidopsis; and the absence of ENs and intermediate numbers of Msh4 foci in budding yeast, where all SC nucleations appear to involve accompanying CO-designation (above; 3, 6, 21, 34, 36, 45). Finally, as suggested by a reviewer, the fact that ENs are less permanently/strongly associated with the SC could be related to the fact that EN-nucleated SC segments are shorter than LN-nucleated segments.

Materials and Methods

Ultrastructural and Hei10 focus data. Analysis of SC and RN patterns (Fig. 2) were performed on previously-described three-dimensional reconstructions (13). Pictures were taken at a magnification of 8000. Three-dimensional reconstructions were performed as follows. The SC elements and nuclear structures from five consecutive sections were traced onto acetate sheets and when the nucleus was completed, each bivalent was redrawn on a new sheet with its relevant section numbers, centromere,

synapsis regions, and nodule sites. The projected lengths were measured and the chromosome lengths were calculated using the Pythagorean theorem (with a mean section thickness of 80 nm). Hei10 T2 and T3 data are from ref. 8.

Beam-film (BF) analysis. BF simulations were performed as described previously (17). Three types of parameters must be specified. (i) The array of precursors is characterized by the average number per bivalent (N), the extent to which those precursors are evenly or randomly spaced along the bivalent (E), the extent to which the number precursors along the bivalent in different nuclei is constant or corresponds to a random distribution (B), and the distribution of intrinsic precursor sensitivities to stress (A). (ii) Patterning parameters include (L), the distance over which the inhibitory interference signal spreads; (Smax), the maximum level of global stress; and cR/cL, which describe the degree of clamping at right and left ends. (iii) Maturation efficiency (M) describes the probability that an event designated to have a particular fate will then mature to the point where it is detected as such by the assay in use. For best-fit simulations of yeast and Sordaria data, the value of (N) is known from experiment (11, 17); precursors are known to be very evenly spaced in Sordaria (11) and also, by several criteria, to be relatively evenly spaced in yeast (17). Maturation efficiencies for yeast and Sordaria are both assumed to be 100% (M=1). For best-fit simulations, approximate values of (L) and (Smax) are defined, after which the values of these and other parameters are adjusted to give the optimal match to CoC and event distribution relationships as judged by visual inspection. Parameter values for best-fit simulations shown here are as follows:

- For CO-correlated Zip3 foci along yeast chromosome XV (Fig. 3*B*): L=0.1 (0.3 μm); Smax=3.5; N=13; A=1; B=1; E=0.6; cL=0.85; cR=0.85.

- For Sordaria T2 foci (Fig. 4 (ii)): L=0.15 (1μm); Smax= 4.5 (corresponding to 1.8 for T3); N=9; A=2; B=0.9; E=0.8; cL=1; cR=1.

- For Sordaria T3 foci, one-round scenario (Fig. 4 (iv)): all parameters the same as for T2 foci except that Smax = 1.8.

- For Sordaria T3 foci, two-round scenario: Precursors are the above-simulated T2 foci (which can also be mimicked with N=5, B=0.9, E=0.8). Based on these precursors, the best-fit simulation of T3 foci uses L=0.205; Smax= 2.8; A=2; cL=1; cR=1.

ACKNOWLEDGMENTS. This work, N.K. and L.Z. were supported by National Institutes of Health grant R01 GM044794. D.Z., E.E., and A.DM. were supported by grants from the Centre National de la Recherche Scientifique (Unité Mixte de Recherche 8621).

References

1. Hunter N (2006) Meiotic recombination. *Molecular Genetics of Recombination,* eds Aguilera A, Rothstein R (Springer Berlin / Heidelberg), pp 381-442.

2. Baudat F, Imai Y, de Massy B (2013) Meiotic recombination in mammals: localization and regulation. *Nat Rev Genet* 14:794-806.

3 Zickler D, Kleckner N (1999) Meiotic chromosomes: integrating structure and function. *Annu Rev Genet* 33:603-754.

4. Muller HJ (1916) The mechanism of crossing over. *Am Nat* 50:193-434.

5. Sturtevant AH (1915) The behavior of the chromosomes as studied through linkage. *Z. indukt. Abstamm.-u. VererbLehre* 13:234-287.

6. von Wettstein D, Rasmussen SW, Holm PB (1984) The synaptonemal complex in genetic segregation. *Annu Rev Genet* 18:331-413.

7. Page SL, Hawley RS (2004) The genetics and molecular biology of the synaptonemal complex. *Annu Rev Cell Dev Biol* 20:525-558.

8. De Muyt A, et al. (2014) E3 ligase Hei10: a multi-faceted structure-based signaling molecule with roles within and beyond meiosis. *Genes Dev* 28:1111-1123.

9. Zhang L, et al. (2014) Topoisomerase II mediates meiotic crossover interference. *Nature* 511: 551–556.

10. Fung JC, Rockmill B, Odell M, Roeder GS (2004) Imposition of crossover interference through the nonrandom distribution of synapsis initiation complexes. *Cell* 116:795–802.

11. Storlazzi A, et al. (2010) Recombination proteins mediate meiotic spatial chromosome organization and pairing. *Cell* 141:94–106.

12. Espagne E, et al. (2011) Sme4 coiled-coil protein mediates synaptonemal complex assembly, recombinosome relocalization, and spindle pole body morphogenesis. *Proc Natl Acad Sci U S A* 108:10614-10619.

13. Zickler D, Moreau PJ, Huynh A D, Slezec AM (1992) Correlation between pairing initiation sites, recombination nodules and meiotic recombination in *Sordaria macrospora*. *Genetics* 132:135–148.

14. Kleckner N (2006) Chiasma formation: chromatin/axis interplay and the role(s) of the synaptonemal complex. *Chromosoma* 115:175-194.

15. Panizza S, et al. (2011) Spo11-accessory proteins link double-strand break sites to the chromosome axis in early meiotic recombination. *Cell* 146:372-383.

16. Berchowitz LE, Copenhaver GP (2010). Genetic interference: don't stand so close to me. *Curr Genomics* 11:91–102.

17. Zhang L, Liang Z, Hutchinson J, Kleckner N (2014) Crossover patterning by the Beam-Film model: analysis and implications. *PLoS Genet* 10: e1004042.

18. Zickler D. (1977) Development of the synaptonemal complex and the "recombination nodules" during meiotic prophase in the seven bivalents of the fungus *Sordaria macrospora Auersw*. Chromosoma 61:289-316.

19. Tesse S, Storlazzi A, Kleckner N, Gargano S, Zickler D (2003) Localization and roles of Ski8p protein in *Sordaria* meiosis and delineation of three mechanistically distinct steps of meiotic homolog juxtaposition. *Proc Natl Acad Sci USA* 100:12865-12870.

20. Kleckner N, et al. (2004) A mechanical basis for chromosome function. *Proc Natl Acad Sci USA* 101:12592-12597.

21. Börner GV, Kleckner N, Hunter N (2004) Crossover/noncrossover differentiation, synaptonemal complex formation, and regulatory surveillance at the leptotene/zygotene transition of meiosis. *Cell* 117:29-45.

22. Terasawa M, et al. (2007) Meiotic recombination-related DNA synthesis and its implications for cross-over and non-cross-over recombinant formation. *Proc Natl Acad Sci USA* 104:5965-5970.

23. Higgins JD, et al. (2012) Spatiotemporal asymmetry of the meiotic program underlies the predominantly distal distribution of meiotic crossovers in barley. *Plant Cell* 24:4096-4109.

24. Phillips D, et al. (2013) Quantitative high resolution mapping of HvMLH3 foci in barley pachytene nuclei reveals a strong distal bias and weak interference. *J Exp Bot*

64:2139-54.

25. De Muyt A, et al. (2012) BLM helicase ortholog Sgs1 is a central regulator of meiotic recombination intermediate metabolism. *Mol Cell* 46:43-53.

26. Blat Y, Protacio RU, Hunter N, Kleckner N (2002) Physical and functional interactions among basic chromosome organizational features govern early steps of meiotic chiasma formation. *Cell* 111:791-802.

27. Qiao H, et al. (2012) Interplay between synaptonemal complex, homologous recombination and centromeres during mammalian meiosis. *PloS Genet* 8:e1002790

28. Lebofsky R, Heilig R, Sonnleitner M, Weissenbach J, Bensimon A (2006) DNA Replication Origin Interference Increases the Spacing between Initiation Events in Human Cells. *Mol Biol Cell* 17:5337-5345.

29. Libuda D E, Uzawa S, Meyer BJ, Villeneuve AM (2013) Meiotic chromosome structures constrain and respond to designation of crossover sites. *Nature* 502:703-706.

30. Anderson LK, Hooker KD, Stack SM (2001) The distribution of early recombination nodules on zygotene bivalents from plants. *Genetics* 159:1259-1269.

31. Lhuissier FG, Offenberg HH, Wittich PE, Vischer NO, Heyting C (2007) The mismatch repair protein MLH1 marks a subset of strongly interfering crossovers in tomato. *Plant Cell* 19: 862-876.

32. Anderson LK, Stack SM (2005) Recombination nodules in plants. *Cytogenet Genome Res* 109: 198-204.

33. Sherman JD, Herickhoff LA, Stack SM (1992) Silver staining two types of meiotic nodules. *Genome* 35:907-915.

34. de Boer E, Stam P, Dietrich AJJ, Pastink A, Heyting C (2006) Two levels of interference in mouse meiotic recombination. *Proc Natl Acad Sci USA* 103:9607–9612.

35. Qiao H, et al. (2014) Antagonistic roles of ubiquitin ligase HEI10 and SUMO ligase RNF212 regulate meiotic recombination. *Nat Genet* 46:194–199.

36. Reynolds A, et al. (2013) RNF212 is a dosage-sensitive regulator of crossing-over during mammalian meiosis. *Nat Genet* 45:269-78.

37. Oliver-Bonet M, Campillo M, Turek PJ, Ko E, Martin RH (2007) Analysis of replication protein A (RPA) in human spermatogenesis. *Mol Hum Reprod* 13:837–844.

38. Bojko M (1985) Human meiosis. IX. Crossing over and chiasma formation in oocytes. *Carlsberg Res Commun* 50:43-72.

39. Ross-Macdonald P, Roeder GS (1994) Mutation of a meiosis-specific MutS homolog decreases crossing over but not mismatch correction. *Cell* 79:1069-1080.

40. Rog O, Dernburg AF (2013) Chromosome pairing and synapsis during *Caenorhabditis elegans* meiosis. *Curr Opin Cell Biol* 25:349-56.

41. Lui DY, Colaiácovo MP (2013) Meiotic development in *Caenorhabditis elegans*. *Adv Exp Med Biol* 757:133-70.

42. Lake CM, Hawley RS (2012) The molecular control of meiotic chromosomal behavior: events in early meiotic prophase in Drosophila oocytes. *Annu Rev Physiol* 74:425-51.

43. Tanneti NS, Landy K, Joyce EF, McKim KS (2011) A pathway for synapsis initiation during zygotene in Drosophila oocytes. *Curr Biol* 21:1852-7.

44. Smolikov S, Schild-Prufert K, Colaiacovo MP (2008) CRA-1 uncovers a double-strand break-dependent pathway promoting the assembly of central region proteins on chromosome axes during *C. elegans* meiosis. *PLoS Genet* 4:e1000088.

45. Higgins JD, Armstrong SJ, Franklin FC, Jones GH (2004) The Arabidopsis MutS homolog AtMSH4 functions at an early step in recombination: evidence for two classes of recombination in Arabidopsis. *Genes Dev* 18:2557-2570.

Figure Legends

Figure 1. Recombinosome and Synaptonemal Complex Morphogenesis in *Sordaria macrospora.* (*A*) Progression of total recombinational interactions as manifested in RNs (ENs, LNs and non-nodule-marked interactions) and two types of Hei10 foci (T2 and T3) in relation to final DNA outcome. (*B*) CoC relationships and the number and distribution of events along bivalents (Biv) 1 and 2 for Hei10-T3 foci and LNs, both of which mark the sites of COs/chiasmata (from ref. 8). (*C*) CoC relationships and the number and distribution of events for Hei10-T2 foci and total RNs (ENs+LNs)

(from ref. 8), both of which correspond to the sites of SC nucleation events as described below. (*D*) Hypothesis for integrated arrays of SC nucleation sites (stripes), LN/CO sites (red circles), EN sites (blue circles) and non-nodule-marked sites (brown bars).

Figure 2. Evidence for a 1:1 Relationship Between SC Nucleation Sites and RNs Sites (ENs+LNs). (*A*) EM pictures of LN (top; 8) and EN (arrows, bottom; 13) nodules. (*B*) 3D ultrastructural reconstruct of a whole mid-zygotene nucleus showing that most bivalents are synapsed at their ends (18). (*C*) Examples of SC (green) and RN (EN in blue, LN in red) patterns along bivalent 1 in reconstructed nuclei: each line corresponds to bivalent 1 in one nucleus. (I, II) Early and mid/late zygotene with progressive SCs plus RNs formation. (III) Early pachytene with full complement of RNs. (IV) Mid/late pachytene nuclei exhibit only LNs due to loss of ENs at early/mid-pachytene. (*D*) Numbers and lengths of all SC segments along bivalents 1+2 that exhibit one of five described morphologies reveal differences in the average and distribution of length: shortest and tightest for SC segments lacking a nodule; longer for segments with a terminal nodule (and among these longer if the nodule is an LN versus an EN); and longest for segments with a single non-terminal nodule (again longer if the nodule is an LN versus an EN). (*E*) Progression of SC nucleation, nodule emergence and SC extension (asymmetric and then symmetric) inferred from length patterns in Panel (*D*). (*F*) All SC segments from bivalents 1+2 that exhibit two RNs were sorted into classes a-f according to nodule type and position (terminal and/or internal). (*G*) Compares the average lengths observed for members of each class with the average lengths predicted on the assumption that the two nodules each exhibited the SC length associated with its corresponding type in Panel (*D*). The two lengths are directly proportional.

Figure 3. Complex Patterning can be Achieved by Reactivity Thresholding in a Single Round of Interference. (*A*) By the logic of the BF model, progressive event-designation results in a progressive decrease in the reactivity of remaining precursors. If the outcome of event designation is different at different levels of reactivity, complex patterns can result. Pictured is a case involving two reactivity thresholds that specify two sequential types of designation outcomes. Below the lower threshold, no event-designation occurs. Patterns can result from the two individual outcomes (1 and 2; pink and brown), which may also include a common component (Total; black). (*B-D*) CoC relationships and the number plus distribution of events for CO-correlated Zip3 foci in

budding yeast - observed (black) and BF best-fit simulation (turquoise) (from ref. 9). Parameters "L" and "Smax" are, respectively, the distance over which the interference signal spreads and the maximum level of global stress, used in simulations to define the total number of event designations (text). Other parameter values given in Materials and Methods. (*E, F*) Under a given set of conditions, including a single specified "interference distance", progressive event designations will result in more and more events that are more and more closely spaced. This outcome is illustrated by BF simulations using the basic best-fit parameters for yeast chromosomes (*B-D*; above) except that the value of Smax is progressively increased. The effects include a shift of CoC relationships to smaller inter-interval distances (*E*) plus an increase in total events (*F*). Note: these effects are analogous to, but have a different basis than, those resulting from "decreased interference" (see discussion in refs 9, 17). (*G-J*) BF modeling of the two-threshold scenario described in (*A*). Outcomes of BF simulations based on yeast parameter values as in (*B-F*), including a fixed value of "L", but with two thresholds defined by appropriate values of Smax (*G*). The number and distribution of events (*H*); corresponding CoC relationships (*I*); and corresponding distributions of distances between adjacent events (*J*) are shown for the first and second types of events and for total events (pink, brown and black, respectively). (*K*) Examples of the patterning outcome from the two-threshold scenario in (*G-J*). An array of relatively evenly-spaced total events (black) includes embedded arrays of events specified by the first and second thresholds (pink and brown, respectively).

Figure 4. Comparison of One-Round and Two-Round Scenarios for Patterning of SC Nucleations and CO Sites in Sordaria.

Left side: Patterns of Hei10-T2 foci, whose sites represent the sites of SC nucleations. Right side: patterns of Hei10-T3 foci, which mark CO sites. Top row: Experimental data (Mer3 foci) define a tight distribution of inter-event distances for total recombinational interactions (*i*, *iii*; ref.11). An analogous distribution of relatively evenly-spaced events was used as the array of total starting precursors for BF simulations for T2 foci (*ii*) and for T3 foci in the one-round scenario (*iv*). The distribution of precursors for the two-round scenario (*v*) is the distribution of T2 foci (*ii*; top middle). Middle two rows: Experimental or predicted distributions of inter-focus distances for T2 or T3 foci for all bivalents (upper) and for the subset of bivalents exhibiting higher numbers of events (lower). Experimentally observed patterns are compared with patterns resulting from BF

best-fit simulations that model different patterning scenarios (panel *i* vs *ii*; panel *iii* vs *iv*, *v*). Two scenarios were examined. (1) A one-round scenario. A single interference process, characterized by a single value for the interference distance "L", gives rise to both T2 and T3 foci, all from the same set of initial precursors. This scenario is qualitatively analogous to the two-threshold case described in Fig. 3*A* and *G-K*. T3 foci correspond to events designated up to the first threshold (Type 1, pink) and T2 foci corresponding to total events that occur up to the second threshold (black). With respect to RNs and SCs, LN-marked sites correspond to Type 1 events; EN-marked sites correspond to Type 2 events; and SC nucleations correspond to total events. (2) A two-rounds scenario in which T2 foci were defined in a first round and T3 foci were defined in a second round for which T2 foci were the precursors. The best-fit simulation of T2 foci is the same in the two cases (panel *ii*). The best-fit simulations for T3 foci give significantly different patterns (panels *iv* and *v*) with a close match between the one-round scenario and the experimental data (panel *iii* versus panel *iv*). Parameter values for best-fit simulations are given in Materials and Methods. Bottom two rows: Experimental or predicted CoC relationships (upper) and number and distribution of events (bottom). Experimental data are shown in green for T2 foci and red for T3 foci. BF best-fit simulation data are shown in black. A peak in T2 or T3 inter-focus distances or a shoulder or hump in CoC relationships at the position of the average inter-focus distance for total precursors (vertical black dashed line) is a diagnostic indicator that the corresponding events arose directly from total precursors (text). This feature should be present for T2 foci by both scenarios. It will be true for T3 foci only by the one-round scenario (middle). For T2 foci, this feature is apparent in both experimental and best-fit simulation data (green arrows). For T3 foci, this feature is apparent in experimental data, thus supporting the one-round scenario. Correspondingly, this feature is also apparent in data for the best-fit simulation of the one-round scenario (red arrows; black circles) and is absent in the best-fit simulation of the two-round scenario (dashed black circle). Further, occurrence of this diagnostic feature in the best-fit simulation of the one-round scenario is dependent upon a tendency for even spacing of precursors: the diagnostic "hump" is absent in the best-fit CoC curve when precursors are assumed to be randomly spaced (Fig. S1).

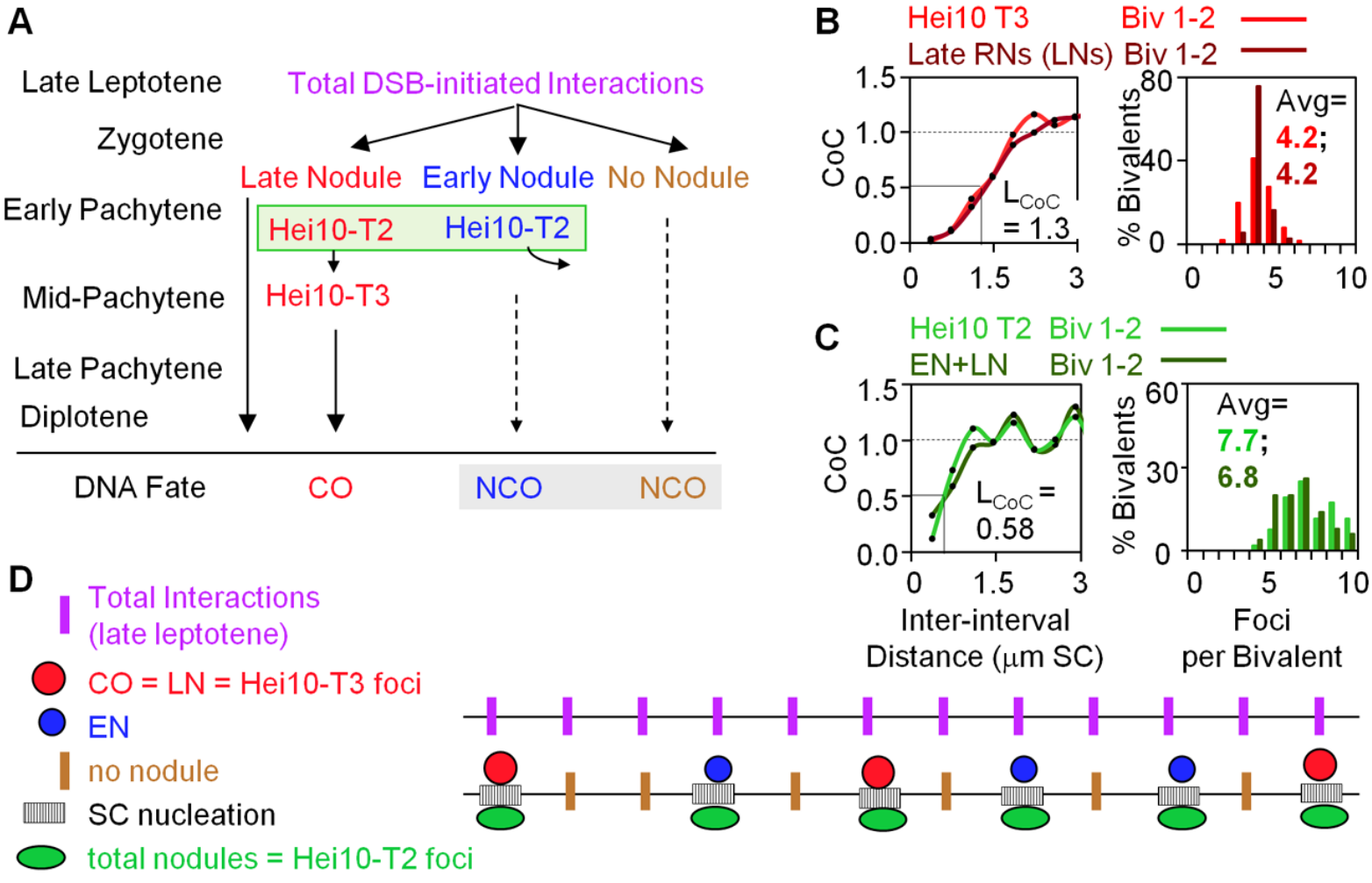
A
Late Leptotene
Zygotene
Early Pachytene
Mid-Pachytene
Late Pachytene
Diplotene
Total DSB-initiated Interactions
Late Nodule
Early Nodule
No Nodule
Hei10-T2
Hei10-T2
Hei10-T3
DNA Fate
CO
NCO
NCO
B
Hei10 T3
Biv 1-2
Late RNs (LNs)
Biv 1-2
CoC
1.5
1.0
0.5
0.0
0
1.5
3
L_{CoC} = 1.3
% Bivalents
80
40
0
0
5
10
Avg=
4.2;
4.2
C
Hei10 T2
Biv 1-2
EN+LN
Biv 1-2
CoC
1.5
1.0
0.5
0.0
0
1.5
3
L_{CoC} = 0.58
Inter-interval Distance (μm SC)
% Bivalents
60
30
0
0
5
10
Avg=
7.7;
6.8
Foci per Bivalent
D
Total Interactions (late leptotene)
CO = LN = Hei10-T3 foci
EN
no nodule
SC nucleation
total nodules = Hei10-T2 foci

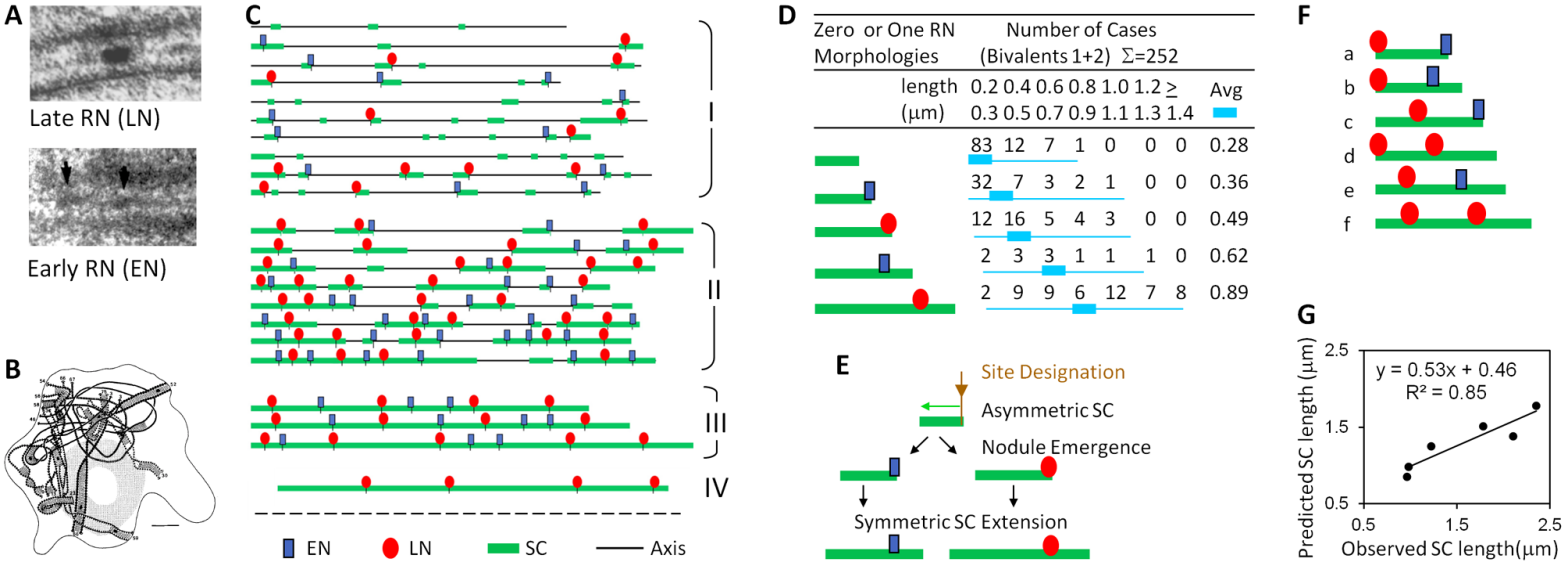
A
Late RN (LN)
Early RN (EN)
B
C
I
II
III
IV
EN
LN
SC
Axis
D
Zero or One RN Morphologies
Number of Cases (Bivalents 1+2) Σ=252
length (μm)
0.2 0.4 0.6 0.8 1.0 1.2 ≥
0.3 0.5 0.7 0.9 1.1 1.3 1.4
Avg
83 12 7 1 0 0 0 0.28
32 7 3 2 1 0 0 0.36
12 16 5 4 3 0 0 0.49
2 3 3 1 1 1 0 0.62
2 9 9 6 12 7 8 0.89
E
Site Designation
Asymmetric SC
Nodule Emergence
Symmetric SC Extension
F
a
b
c
d
e
f
G
y = 0.53x + 0.46
R² = 0.85
Predicted SC length (μm)
Observed SC length(μm)
0.5
1.5
2.5

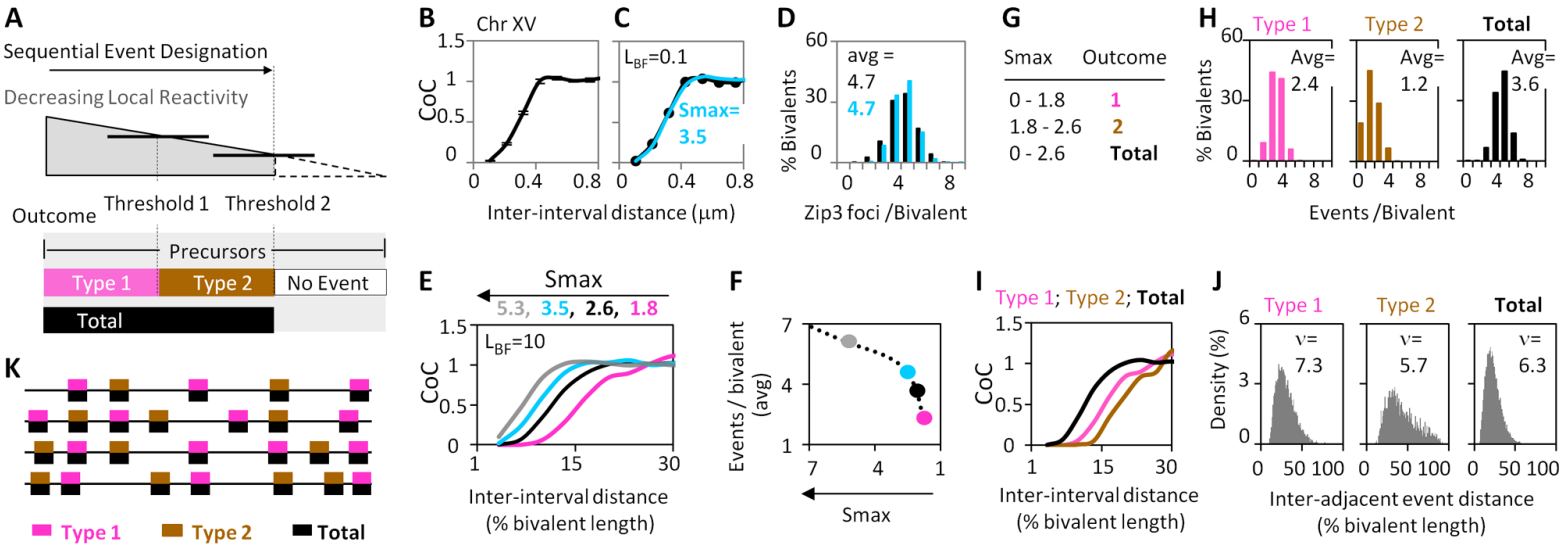
A
Sequential Event Designation
Decreasing Local Reactivity
Threshold 1
Threshold 2
Outcome
Precursors
Type 1
Type 2
No Event
Total
B
Chr XV
CoC
Inter-interval distance (μm)
C
L_BF=0.1
Smax=
3.5
D
avg =
4.7
4.7
% Bivalents
Zip3 foci /Bivalent
G
Smax
Outcome
0 - 1.8
1
1.8 - 2.6
2
0 - 2.6
Total
H
Type 1
Type 2
Total
Avg=
2.4
1.2
3.6
% Bivalents
Events /Bivalent
E
Smax
5.3, 3.5, 2.6, 1.8
L_BF=10
CoC
Inter-interval distance
(% bivalent length)
F
Events / bivalent
(avg)
Smax
I
Type 1; Type 2; Total
CoC
Inter-interval distance
(% bivalent length)
J
Type 1
Type 2
Total
ν=
7.3
5.7
6.3
Density (%)
Inter-adjacent event distance
(% bivalent length)
K
Type 1
Type 2
Total

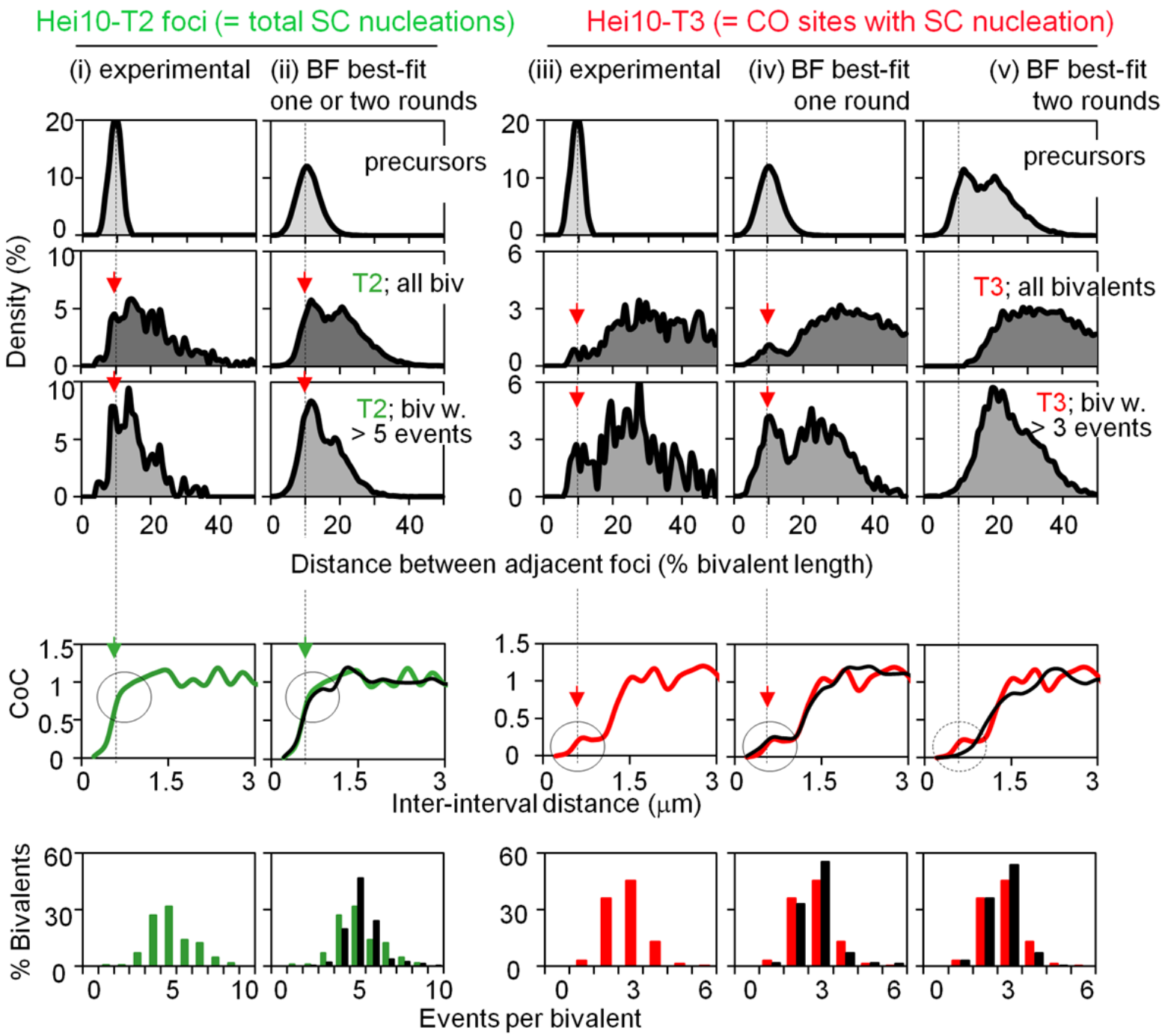
Hei10-T2 foci (= total SC nucleations)
Hei10-T3 (= CO sites with SC nucleation)
(i) experimental
(ii) BF best-fit one or two rounds
(iii) experimental
(iv) BF best-fit one round
(v) BF best-fit two rounds
precursors
T2; all biv
T2; biv w. > 5 events
T3; all bivalents
T3; biv w. > 3 events
Density (%)
Distance between adjacent foci (% bivalent length)
CoC
Inter-interval distance (μm)
% Bivalents
Events per bivalent